

Electric Vehicle Electromagnetic Compatibility Testing and Electromagnetic Emission Mitigations

Sunay GÜLER

Abstract: Amidst the rapidly evolving landscape of road transportation, the imperative for sustainable and eco-friendly solutions is underscored by global regulations aimed at reducing CO₂ emissions from vehicles. This heightened global awareness thrusts electric vehicles (EVs) into the forefront. While transitioning to EVs promises a reduction in CO₂ emissions compared to conventional vehicles, it also raises concerns regarding electromagnetic compatibility (EMC) assurance. This study initiates by examining electromagnetic compatibility standards and testing requirements for electric vehicles. Then, technical approaches and critical factors such as grounding strategy, cable routing considerations and electromagnetic shielding to mitigate electromagnetic emissions are investigated. After that, vehicle-level EMC testing and assessment of electromagnetic emissions from an electric vehicle is conducted, in compliance with UNECE regulation no. 10. Radiated and conducted emissions are measured during EV charging by following CISPR 12 standard. It is obtained that the measurements of emission testing conform to the specified limits delineated in CISPR 12. Consequently, the electric vehicle under examination successfully meets both radiated and conducted emissions requirements.

Keywords: conducted emission; electric vehicle; electromagnetic compatibility; electromagnetic interference mitigations; radiated emission; vehicle-level testing

1 INTRODUCTION

In the rapidly evolving road transportation, sustainable and eco-friendly solutions have become mandatory due to the global regulations reducing CO₂ emission of the vehicles. The surge in global awareness about reduction of CO₂ emission has propelled electric vehicles (EVs) into the spotlight. As industries and consumers increasingly recognize the emphasis of sustainable transportation, the demand for EVs has seen unprecedented growth. Vehicle market global forecast indicates that the number of electric vehicles will be increased significantly and the grow rate of EV market is expected as 13.7% from 2023 to 2030 [1].

Utilizing EVs for the road transportation will definitely degrade the level of CO₂ emission produced by conventional vehicles, yet it will bring concerns regarding the assurance of electromagnetic compatibility (EMC) against electromagnetic interference (EMI) [2, 3]. In general, EMC is defined as the capability of an electronic equipment or a system to be operated in the intended electromagnetic environment at design levels of efficiency [4]. Advanced driver assistance systems (ADAS) and autonomous driving technologies have already been applied to the vehicles increasingly over the last decade. In addition to this intricate environment, EVs integrate electrified powertrain systems supplied by high-voltage batteries. Assuring EMC for EVs and their subsystems within these environments becomes a critical issue, starting from the vehicle's design phase and extending throughout its series production [5, 6].

Electromagnetic compatibility of the vehicle can be assured by following two main types of EMC tests which are EMC emission tests and EMC immunity tests, respectively [7]. EMC emission tests are divided into subcategories such as radiated and conducted emission tests and cover both vehicle-level and component-level testing. Radiated emission tests are performed based on broadband and narrowband emissions [8]. On the other hand, EMC immunity tests investigate how radiated or conducted emissions affect the entire vehicle electrical and electronic (E&E) systems. Similarly, they are divided into two categories such as vehicle-level and component-level

immunity tests, aimed at verifying the operability of the vehicle or any E&E component without compromising performance in their intended environment.

Since EVs and their subsystems create more complex environment, emission and immunity characteristics upon vehicle-level and component-level should be comprehended and managed carefully. In addition, electrostatic discharge (ESD) immunity and immunity to transient voltage need to be investigated to assure EMC of the electric vehicle. To ensure electromagnetic compatibility for EVs, it is essential to adhere to EMC standards and testing requirements [3].

Based on the literature review, some EMC standards following for EMC testing of EVs are reported [3]. EMC tests for EVs according to European standards are presented [6]. Available regulations and standards on EVs charging through wireless power transfer are investigated [9]. Each regulation is outlined separately, followed by a comparative discussion focusing primarily on electromagnetic compatibility. Radiated emission performance at electronic sub-assembly level at different e-machine loading conditions and test setup cases is carried out [10]. A methodology is introduced to predict vehicle-level radiated EMI by using multiple network theory [11]. The basics of electromagnetic compatibility testing of electric vehicles and electric vehicle chargers in accordance to current EMC standards are presented [12]. The challenges of testing high voltage systems of modern electric and hybrid vehicles for electromagnetic compatibility are carried out [13]. The draft version of the International Electrotechnical Commission (IEC) 61851-21-2, an EMC standard for conductive charging infrastructure, is examined in detail. Critical issues related to diverse charging modes and specialized interfaces to energy supply networks are highlighted. [14]. Radiated emissions of an EV is investigated depending on the different operating modes [15].

In this study, electromagnetic compatibility standards and requirements for testing EVs are carried out at first. Then, technical approaches to mitigate electromagnetic emissions at design phase are investigated and critical factors are highlighted to improve EMC performance of the

vehicle. After that, vehicle-level electromagnetic emissions testing and assessment of an electric vehicle based on regulation no. 10 of the United Nations Economic Commission for Europe (UNECE) are presented. Several studies can be reported for the investigation of vehicle EMC tests upon the literature review [3, 6, 11]. However, there are limited number of studies which examine technical approaches for emission mitigations before performing vehicle-level EMC testing. This study uniquely bridges theoretical EMC design methods with regulatory vehicle-level validation by focusing on real EV architecture and standardized emission testing.

The reminder of this study is as follows. Section 2 covers EMC standards and requirements for the electric vehicles. Section 3 carries out all EMC test setups based on UNECE regulation no. 10. Section 4 gives technical approaches and critical factors to mitigate electromagnetic emissions of the vehicle. Section 5 presents the measurement results of radiated and conducted emissions. Finally, the concluding remarks are included in Section 6.

2 EMC STANDARDS FOR EV

There are worldwide organizations which aim to enforce EMC regulations for the vehicles and their E&E systems such as International Special Committee on Radio Interference (CISPR), International Organization for Standardization (ISO), Society of Automotive Engineers (SAE) and IEC. Currently, EMC requirements and EMC test methodologies for EV type approval are carried out according to UNECE regulation no. 10 which takes into account EVs and their E&E systems as a whole. Besides that, EV charging infrastructure is regulated by IEC standards depending on on-board and off-board chargers [12].

Tab. 1 shows EMC tests based on global EMC standards mentioned in UNECE regulation no. 10, which must be passed before applying the vehicle type approval.

Table 1 EMC tests and standards for EVs

EMC Tests	Test Standards
Radiated emission	CISPR 12
Conducted emission	
Radiated, radio frequency, electromagnetic field immunity	IEC 61000-4-3
Electrical fast transient immunity	IEC 61000-4-4
Surge immunity	IEC 61000-4-5
Voltage variations and flicker	IEC 61000-3-3
Harmonics	IEC 61000-3-2

3 VEHICLE-LEVEL EMC TESTING

EVs have electrified powertrain supplied by high voltage (HV) battery pack that is the most critical part in terms of electromagnetic compatibility. Switching on transistors of the inverter unit may cause voltage surge that can affect E&E systems of the entire vehicle since it generates radiated and conducted emissions. e-Machine is the core component of electrified powertrain systems since it has significant impact on power, architecture, cost and reliability of the vehicle [16]. The vehicle under test (VUT) has an electrified powertrain architecture as shown in Fig. 1. Tab. 2 presents the components of the electrified powertrain along with their specifications. Almost every

E&E system includes low-voltage circuits that are sensitive to EMI. Besides that, ADAS and infotainment systems broadcast signals at various frequencies, which also create additional EMI inside the vehicle environment. Therefore, it is crucial to protect the systems against external EMI and minimize the interference generated by the systems themselves. EMI can occur electrically, magnetically, or through radiation, depending on the sources. Only complete EMC tests according to UNECE regulation no. 10 can conclusively determine EMC status of the entire vehicle and its E&E systems. In this study, all tests are conducted in anechoic chamber at an ISO/IEC 17025-accredited EMC test facility. Measurements are taken by using a calibrated EMI receiver (Rohde & Schwarz ESCI) with biconical and log-periodic antennas covering the 30 MHz - 1 GHz range.

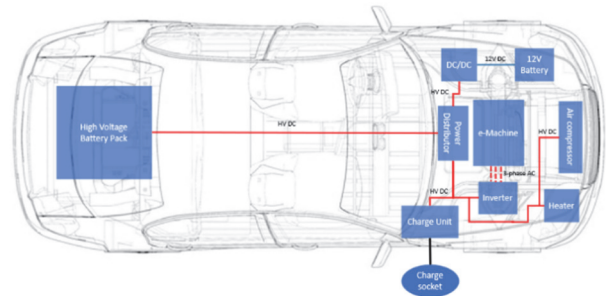


Figure 1 Electrified powertrain inside EV

Table 2 The component specifications of e-powertrain

Component	Specification
e-Machine	Max Power: 100 kW / 134 HP Torque: 234 Nm
Battery	Lithium-ion cells, Capacity: 70 kWh
Inverter	Max. Operating Voltage: 116 VDC Min. Operating Voltage: 39.1 VDC
Charger	Rated Output Power: 6.6 kW Input Voltage Range: 90-456 VAC
DC/DC Converter	Rated Output Power: 2.8 kW Input Voltage: 30 -1500 V
PTC Heater	Rated Output Power: 6 kW Max. Operating Voltage: 450 V

The following subsections provide a comprehensive overview of the vehicle-level EMC testing procedures performed on the VUT, in accordance with CISPR 12 and UNECE Regulation No. 10. These tests are grouped into two main categories: emission tests, which assess the vehicle's electromagnetic emissions (Sections 3.1 and 3.2), and immunity tests, which evaluate the vehicle's resilience to external electromagnetic fields and surges (Sections 3.3 and 3.4).

3.1 Radiated Emission Testing

Radiated emission testing under CISPR 12 is conducted within the frequency range of 30 MHz to 1 GHz. VUT is supplied by 230 V AC in anechoic chamber during testing. Test is performed by turning VUT right and left directions while receiving antenna has vertical and horizontal polarizations. Two operating conditions of the vehicle are considered during radiated emission testing which are key-on & engine-off condition and driving the vehicle at the constant speed of 50 km/h condition,

respectively. Test setup for radiated emission testing is depicted in Fig. 2.

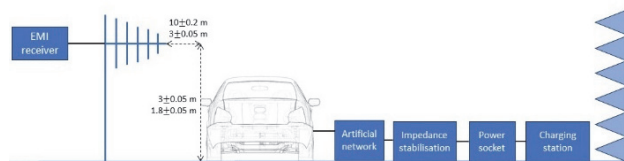


Figure 2 Radiated emission testing

Any facility to perform radiated emission testing should include various antennas for the specific frequency bandwidth such as biconical, log-periodic or broadband antennas, EMI receiver, anechoic chamber. During the radiated emission measurement, receiving antennas should be located 3 m distance from the vehicle.

While measuring the radiated emission during vehicle charging mode, charging cable should be connected to the vehicle via artificial network and impedance stabilization network. EVs should have state of charge (SoC) between 20% and 80% during the measurements [6].

3.2 Conducted Emission Testing

In conducted emission testing, a product undergoes examination for radio-frequency voltage noise it generates on a conductive medium. This medium could be multi-wire connectors handling communication signals or power line cables serving as power supply conduits. Such disturbances often originate from sources like rectifiers within AC to DC power supply systems and have the potential to interfere with the operation of other components along the cabling system [17]. Moreover, given the communication systems between electric vehicles and their chargers, it is imperative to assess conducted emission levels from the telecommunication ports of both the EV and the charger.

Fig. 3 illustrates test setup configuration for conducted emission testing while a vehicle is charged. In this configuration, EV is connected to a Line Impedance Stabilization Network (LISN), also referred to as an Artificial Mains Network (AMN). The LISN is then linked either to a charging station or directly to a power mains socket.

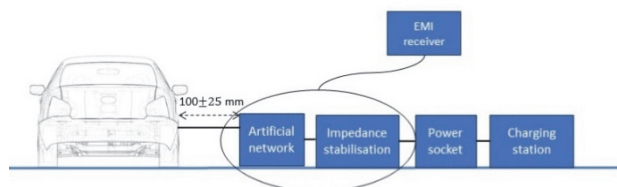


Figure 3 Conducted emission testing

According to UNECE Regulation No. 10, the quasi-peak and average measurement levels are compared against predefined limits to ensure compliance. This testing procedure is designed to assess the level of radio frequency conducted disturbances emitted from vehicles during charging mode, with the aim of verifying

compatibility with residential, commercial and light industrial environments.

Conversely, electric vehicles have the potential to generate harmonics via their AC power lines. Additionally, fluctuations in voltage and flickering may occur along AC power lines of EVs. EMC standards outline the methods for measuring harmonic and flicker emission levels, specifying that such tests should be conducted during the charging mode of EVs. Throughout the conducted emission tests, EV must remain immobilized with the engine turned off. Moreover, any equipment that can be permanently activated by the driver or passenger must be switched off.

3.3 Radiated Immunity Testing

EVs must demonstrate resilience to radiated electromagnetic fields throughout various operational modes. These fields are applied to EVs both during charging and other modes of operation. During charging mode tests, the vehicle must be stationary with the engine off. Conversely, for tests conducted during other modes than charging, the vehicle should maintain a constant speed of 50 km/h, with additional repetitions performed under brake cycle mode. Throughout these tests, all equipment permanently switchable by the driver or passenger must remain on. The test setup for charging mode is depicted in Fig. 4.

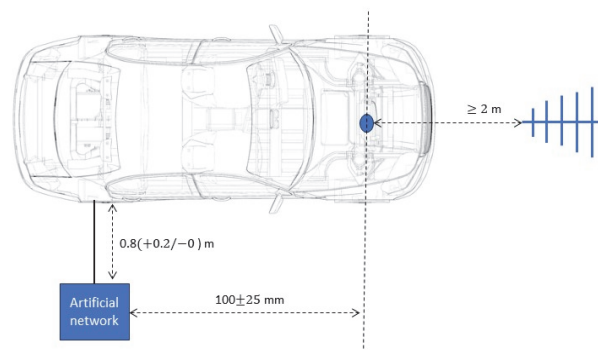


Figure 4 Radiated immunity testing during charging mode

3.4 Conducted Immunity Testing

The electronic systems of EVs must demonstrate immunity to disturbances conducted along both AC and DC power lines, necessitating comprehensive testing procedures. During EV charging mode, EV is subjected to electrical fast transient disturbances and surges. EV shall be immobilized while all permanently switchable equipment shall be turned off. Continuous monitoring of EV is conducted throughout the tests. Electrical surges are applied by using a coupling/decoupling network (CDN) between each line and earth, as well as between lines. The surge test setup, depicted in Fig. 5, incorporates surge levels of ± 500 V for DC power lines and ± 1000 V (L-L) and ± 2000 V (L-P) for AC power lines. Surge tests are applied across all phases (0° , 90° , 180° , 270°). Additionally, electrical fast transient tests are performed on power lines in common modes with burst levels set at ± 2000 V for both AC and DC power lines. The test configuration is depicted in Fig. 5.

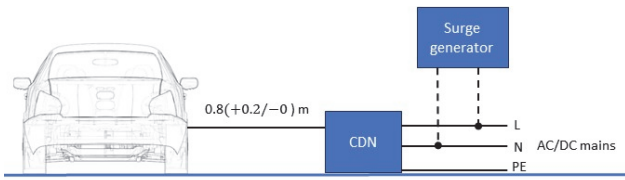


Figure 5 Surge immunity testing

4 EMISSION MITIGATIONS

Reducing electromagnetic emissions in automotive remains a substantial challenge since the industry advances towards more sophisticated and integrated vehicle E&E architectures. This study explores technical approaches to mitigate electromagnetic emissions and highlights critical factors to improve EMC performance of VUT before performing vehicle-level EMC testing.

4.1 Grounding Strategy

Proper grounding is fundamental to reduce electromagnetic emissions. Ensuring low-impedance connections by enhancing grounding systems attenuates the propagation of EMI. Techniques such as star grounding and utilizing ground planes minimize ground loops and reduce potential differences which lead to EMI. Ground planes also act as a screen providing low-impedance connections. Multi-layer Printed Circuit Board (PCB)

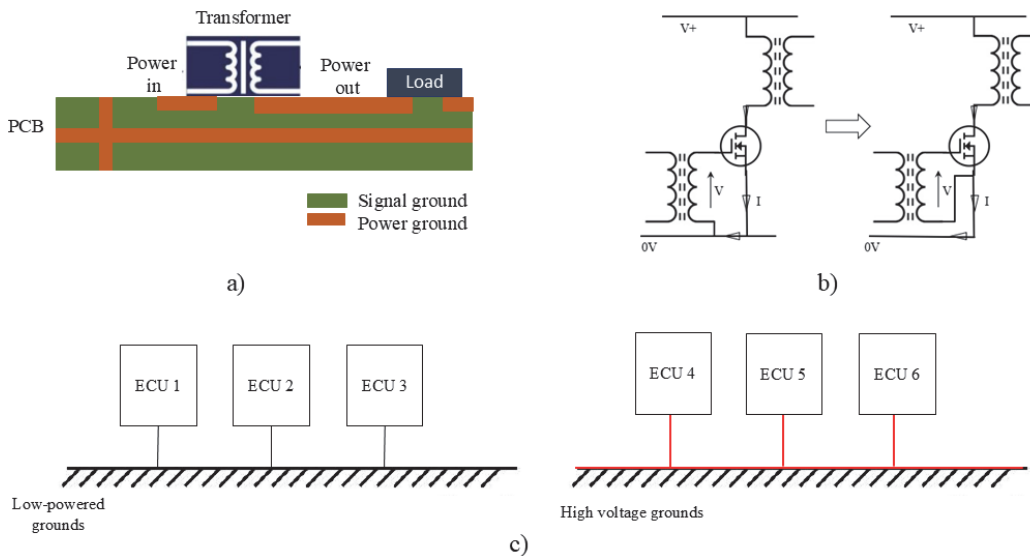


Figure 6 Grounding guidelines: a) multi-layer PCB with ground planes, b) method of avoiding faulty turn-on cycles caused by wiring inductance in circuits, c) multi-point grounding

4.2 Cable Routing Considerations

Wiring harness design and routing cables are critical factors in controlling electromagnetic emissions. Routing of cables must be designed to avoid parallel runs with high-power or high-frequency lines. Adequate separation between sensitive signal cables and noise-generating components must be maintained.

For minimizing the effect of low-frequency EMI, susceptible wires should be routed as far as possible from power sources and HV cables as shown in Fig. 7a. Fig. 7b depicts that when wires must cross, they should do so at right angles and any parallel wires should be kept as far apart as possible to reduce coupling. These general design

principles help in avoiding unwanted EMI pickup, particularly in vehicles where power and signal cables coexist.

design offers flexibility for wiring and component placement by allowing multiple layers of conductive paths within a compact structure as shown in Fig. 6a. It also illustrates the importance of establishing consistent and reliable bonding for all E&E components inside any electrical control units (ECUs) of the vehicle.

Determining grounding points is crucial to avoid issues such as voltage drops caused by inductance in common wires. For instance, if the gate of a Metal-Oxide-Silicon Field Effect Transistor (MOSFET) is connected through a shared wire carrying source current as shown in Fig. 6b, the inductive effect at high switching frequencies can cause significant voltage drops. This can result in faulty turn-on cycles of the MOSFET. By directly connecting the transformer to the source of the transistor, these issues can be avoided and ensures reliable operation of the switching circuit [18].

In practice, adhering strictly to a single grounding scheme can be difficult, so the following guidelines can help to mitigate electromagnetic emissions which are also adopted for VUT depicted in Fig. 6c:

- Avoid mixing noisy, high-power circuit grounds with low-power signal grounds.
- Use separate grounds for chassis and AC power.
- Keep high-power ground leads as short as possible to minimize interference.

finite-length current filament under these conditions. For an x -directed wire of length $2L$ which is centered at the origin of the coordinate system, the magnetic flux density $\vec{B}(r, I, L)$ at a point r generated by a steady current I is obtained by Eq. (1).

$$\vec{B}(r, I, L) = \frac{\mu_0 I}{4\pi(y^2 + x^2)} \left\{ \frac{L+x}{\sqrt{(L+x)^2 + y^2 + x^2}} + \frac{L-x}{\sqrt{(L-x)^2 + y^2 + x^2}} \right\} (-z\hat{y} + y\hat{z}) \quad (1)$$

where \hat{y} and \hat{z} represents unit vectors in y and z directions, respectively, while $\mu_0 = 4\pi \times 10^{-7}$ H/m is the magnetic permeability of free space and steady current is defined as $I = 1$ A.

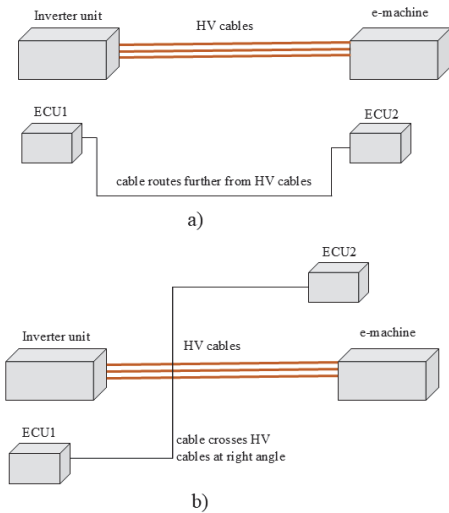


Figure 7 Better cable routings: a) Parallel cable routing, b) crossing HV cables at right angle

Three-phase HV power cables in electric vehicles are typically arranged in flat configurations as illustrated in Fig. 7 to connect e-machine to the inverter. However, the trefoil configuration can offer significant advantage in reducing stray magnetic fields compared to the flat configuration. Fig. 8 depicts both flat and trefoil configurations for three-phase power cables. It is assumed that the conductors carry currents with phases of $0, 2\pi/3$ and $4\pi/3$ radians with a spacing of 2 cm between current paths.

Tab. 3 presents the result of calculations by adopting Eq. (1) for both flat and trefoil configurations at some observation points while the wire of length $2L = 2$ m and a spacing of 2 cm between current paths. The results show that the trefoil configuration decreases magnetic fields compared to flat configuration which makes it more effective in mitigating electromagnetic emissions within the vehicle. The magnetic field reduction achieved with the trefoil cable layout is consistent with findings reported in the literature [19-21]. The results similarly show improved cancellation of magnetic flux in the cabin region, although the exact improvement varies depending on observation point and distance from the cable.

Although the trefoil cable configuration demonstrates better magnetic field cancellation from a theoretical standpoint, its implementation in production vehicles poses several challenges. Trefoil cable layouts tend to be stiffer because of their tightly grouped structure, which makes them harder to route through sharp bends, narrow passages or tight packaging areas commonly found in vehicle architectures. Additionally, the circular cross-section of trefoil arrangements occupies more space than flat harnesses, potentially conflicting with design constraints in areas such as battery tunnels, rocker panels. These practical limitations must be weighed against EMC performance benefits during the vehicle's electrical architecture design phase.

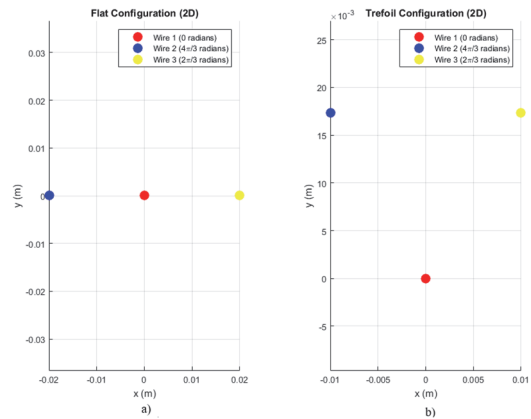


Figure 8 Three-phase power cable: a) flat configuration, b) trefoil configuration

Table 3 Calculated results for 2 m long three-phase cable with 2 cm spacing between current paths

Observation point	Observation point coordinates / mm			Net magnetic flux density / nT	
	x	y	z	Flat	Trefoil
Seat	35	-400	-370	1777	1745
Trunk	140	-340	-70	1450	1422
Head	250	-420	380	1215	1196

4.3 Electromagnetic shielding

Electromagnetic shielding is crucial in reducing radiated emissions of EV power electronic units such as inverters, converters and e-machine controllers which generate significant EMI due to their high frequency switching and large currents they handle. This EMI can radiate into the surrounding environment therefore it can interfere with the operation of systems such as electrified powertrain, infotainment and ADAS.

Electromagnetic shielding enclosures help contain radiated emissions by blocking unwanted electromagnetic waves. One of the main challenges is the need for aperture or thin slots in the enclosure walls due to ventilation, access to connectors or cable pass-throughs, which can attenuate the shielding performance of the enclosure. To mitigate this, careful design for the apertures is essential. Shielding performance of the enclosure is determined by shielding effectiveness (SE) which calculates the reduction of electromagnetic fields thanks to the presence of the shielding enclosure. SE at point P is calculated by:

$$SE = 20 \log \left| \frac{\vec{E}_1(p)}{\vec{E}_2(p)} \right| \quad (2)$$

where $\vec{E}_1(p)$ represents the electric field measured in the absence of the shielding enclosure and $\vec{E}_2(p)$ denotes the electric field measured when the enclosure is present [22].

In addition to precise design of HV power cables routing and their configurations, it is equally essential to carefully design the enclosure apertures for cable pass-throughs to ensure optimal performance. In automotive applications, cable pass-throughs can have different shapes to accommodate different cable types and configurations. Rectangular and square apertures are frequently utilized for multiple cables or connectors while circular apertures are common for individual cables or round connectors but they provide a tight fit. Besides this, some shielding enclosures can have custom-shaped apertures for specific connector types or cable assemblies which offer a balance between accessibility and electromagnetic shielding.

Fig. 9 illustrates an electromagnetic shielding enclosure of an inverter unit which is designed in CST to analyse the effect of aperture shapes on SE. 3433 tetrahedrons are used to build the enclosure mesh and for the electromagnetic simulation, frequency domain solver is utilized. Material of the enclosure is selected as aluminium. The enclosure dimensions are defined as 227 mm in length, 78 mm in width, 168 mm in depth and 2.5 mm in thickness of the enclosure wall which is compatible with the dimensions of inverter unit in VUT. Three identical apertures, each with an area of 3.14 cm² and spaced 1 cm apart, are placed on the front panel of the enclosure and their shapes vary as circular, rectangular and square for three different conditions.

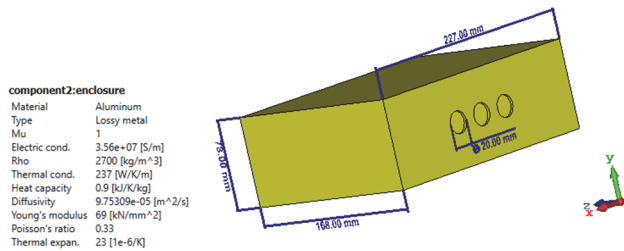


Figure 9 Enclosure model built in CST

The structure is illuminated by an incident plane wave propagating along the +z-axis with polarization in the y-direction. The frequency range considered is 0-2 GHz and the amplitude of the electric field is defined as $|E| = E_y = 1$ V/m. Problem space is modelled as free space with conductivity $\sigma = 0$ S/m. Electric field distributions are calculated at the observation point P , located at the geometric center of the enclosure. Fig. 10 presents a comparison of SE results for different aperture shapes.

From Fig. 10, it is observed that the best SE results are achieved with 3 square apertures while 3 rectangular apertures yield the worst SE performance. At 400 MHz frequency sample point, the SE of the square aperture configuration is 8 dB higher than the circular configuration while the SE of the circular configuration is 10 dB higher than the rectangular configuration. This improvement is attributed to the symmetric geometry of square apertures, which helps to distribute surface currents more uniformly and minimize resonant coupling with incident electromagnetic waves. In contrast, rectangular apertures

with longer edges tend to act as slot antennas. It is obtained that unless there is a specific reason, square apertures are preferable for the accommodation of three-phase power cables and they should be sealed with grommets or conductive materials to maintain electromagnetic shielding.

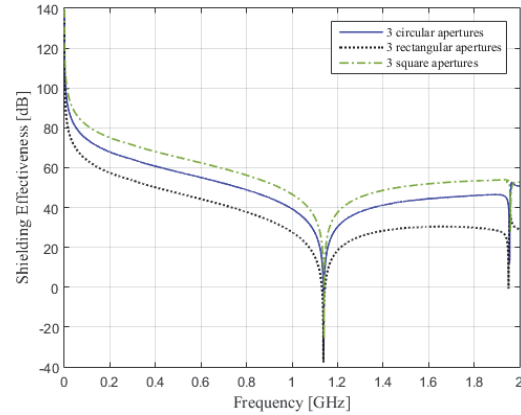


Figure 10 Comparison of SE results for different aperture shapes

The CST simulation results on shielding effectiveness are aligned with prior studies in the literature [21, 22], which show that square apertures yield more uniform current distribution and lower coupling efficiency than other slots. Our study confirms this behaviour and extends it to a practical EV inverter geometry, reinforcing the general applicability of aperture-shape optimization in automotive enclosures.

Unlike most studies that focus on component-level or simulation-only validation, this study presents a holistic approach by applying design-phase emission mitigation techniques and validating their effectiveness at the vehicle-level through standardized EMC tests. Tab. 4 highlights the engineering trade-offs associated with key EMC mitigation techniques investigated in this study.

Table 4 Trade-offs between EMC effectiveness and practical considerations for design-phase mitigations

Mitigation Technique	EMC Impact	Installation Complexity	Flexibility	Cost
Ground plane design	Medium	Low	High	Low
Trefoil configuration	High	High	Low	Moderate
Enclosure with square aperture	High	Low	High	Low

5 VEHICLE-LEVEL EMC TEST RESULTS

Radiated emission testing is conducted based on CISPR 12 standard by locating a receiving antenna 3 meters away from the vehicle. The vehicle is supplied with 230 V AC in anechoic chamber while measuring radiated emissions. The receiving antenna is utilized to measure induced voltage for both key-on & engine-off condition and driving the vehicle at the constant speed of 50 km/h condition. A Rohde-Schwarz ESCI EMI test receiver serves as a spectrum analyser for capturing field strength data from the antenna. Biconical antenna is utilized during the measurement between 30 - 300 MHz frequencies while log-periodic antenna is used for the frequency range of 300 MHz to 1 GHz.

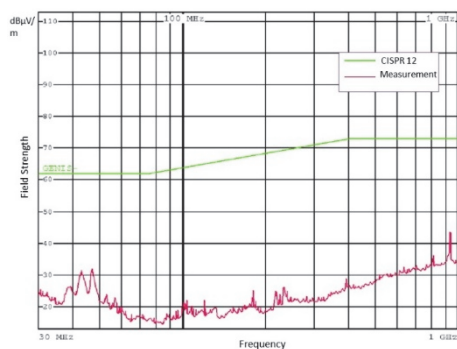


Figure 11 Measurement of radiated emissions with a vertically polarized receiving antenna during the key-on & engine-off status

Fig. 11 shows the field strength of radiated emissions while the receiving antenna is located on the left-hand side of VUT having vertical polarization. The vehicle condition is key-on & engine-off during the measurement. It is observed that radiated emission is significantly lower when the e-machine is turned off. There is no notable peak based on the receiving antenna voltage across a wide frequency band. However, an instant peak is observed around 1 GHz, with field strength of 43.7 dB μ V, which remains significantly below the defined regulatory threshold. The limit line shown in green in Fig. 11 rises up to \sim 74 dB μ V/m, which exceeds the standard CISPR 12 limit for a 3-meter test (approximately 64.5 dB μ V/m). This threshold likely reflects OEM (Original Equipment Manufacturer) - specific EMC acceptance criteria for 3 m test distances.

Fig. 12 illustrates the field strength of radiated emissions while the receiving antenna is located on the left-hand side of VUT and the vehicle is driven on the roller dynamometer at the constant speed of 50 km/h.

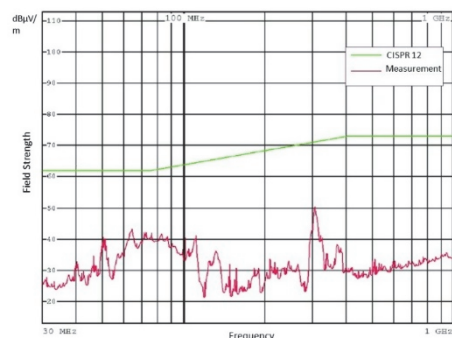


Figure 12 Measuring radiated emissions with a vertically polarized receiving antenna while driving the vehicle at a constant speed of 50 km/h

During driving VUT with the constant speed of 50 km/h, multiple instantaneous peaks are observed, with the highest peak occurring around 300 MHz and reaching a field strength of 50.3 dB μ V. They indicate the broadband radiated emissions since they are mainly caused by the electrified powertrain system. Both results obtained by Fig. 11 and Fig. 12 remain within the specified limits based on CISPR 12.

Measurements can utilize quasi-peak or peak detectors for broadband emissions, whereas narrowband emissions are typically assessed with average detectors. Broadband and narrowband emissions refer to emissions with bandwidths greater or less than that of a specific measuring apparatus or receiver. Fig. 13 shows measuring

narrowband radiated emissions with a vertically polarized receiving antenna during the key-on & engine-off status.

The narrowband radiated emissions from vehicles may originate from sources such as microprocessor-based systems or other narrowband devices. It is observed that the measurement is quite lower and there is no notable peak based on the specified limit. The highest peak occurring around 1 GHz and reaching a field strength of 23.8 dB μ V is shown in Fig. 13.

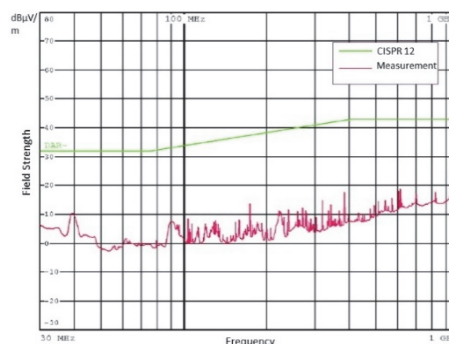


Figure 13 Measurement of narrowband radiated emissions with a vertically polarized receiving antenna during the key-on & engine-off status

E&E systems may generate electromagnetic noise that travels through the power supply inside EVs. Hence, it is crucial to isolate this electromagnetic noise and other disturbances. LISN is employed to establish standard impedance and filter out any incoming noise from the main power supply, ensuring clean power for VUT. Measured conducted emissions are compared with EMC limits specified for the frequency band in the relevant standards, frequency by frequency. Fig. 14 illustrates the measurement of conducted emissions, displaying peak values in dB μ V between 150 kHz and 30 MHz, alongside average (AV) and quasi-peak (QP) limits.

Fig. 14 portrays the full spectrum graph of the measurement of conducted emissions. The figure points out some average peak values, denoted by the solid black line while solid blue line indicates the average limit upon CISPR 12. The highest average value is measured as 41.78 dB μ V at 153 kHz.

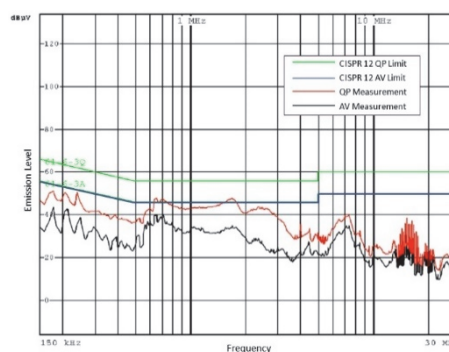


Figure 14 Measurement of conducted emissions including both quasi-peak and average peak values

6 CONCLUSIONS

Because of the intricate EMI environment of electric vehicles, ensuring EMC becomes a crucial concern, starting from the early design phase and extending through series production. The electrified powertrain system stands

out as the most critical part of EVs in terms of EMC since it generates radiated and conducted electromagnetic emissions within its environment, impacting both the vehicle's operation and human safety.

This study presents a structured approach to vehicle-level EMC assessment and mitigation strategies for EVs, in alignment with UNECE regulation no. 10 and CISPR 12 standards. A combination of design-phase methods, such as ground strategy, optimized cable routing and enclosure-level shielding enhancements, is investigated through theoretical and simulation-based analyses. Shielding effectiveness is evaluated by using CST simulations that model aperture geometry and material properties representative of real automotive enclosures. The results show measurable improvements in shielding performance when using square-shaped apertures. Magnetic field reduction in trefoil cable layouts is validated by using the Biot-Savart Law. Radiated and conducted emission measurements are performed under standardized test conditions and confirmed compliance with regulatory limits across all vehicle operating modes.

While the study provides practical insight into mitigation strategy effectiveness, some constraints such as the scope of physical testing for individual design features limit further experimental correlation. While the approach offers clear benefits, the proposed trefoil cable configuration may not always be practical since it is less flexible compared to flat configuration and can be challenging to install within the vehicle. Square or rectangular apertures are often used for the enclosures although some enclosures still have custom-shaped apertures for specific connector types or cable assemblies which offer a balance between accessibility and EMI shielding. Consequently, despite providing some guidelines in this study, it is worth noting that vehicle specific guidelines are not possible due to diversity of electrified powertrain systems in the automotive industry. Performing design reviews at the initial phase of development can identify potential EMI issues and help to obtain proactive mitigation plans. Designing all E&E subsystems based on EMC standards and integrating them cohesively prevent EMI issues at component-level.

Future work will focus on validating shielding and cabling strategies through hardware implementation and expanded testing under transient and immunity conditions, including ESD and load dump events in high-voltage vehicle platforms.

7 REFERENCES

- [1] Lauko, R. (2024). Electric vehicle charging services perspectives and challenges. *Proceedings of the International Conference on Business Excellence*, 18(1), 2548-2561. <https://doi.org/10.2478/picbe-2024-0214>
- [2] Widek P. & Alaküla, M. (2023). Common mode current measurements in traction systems for electric vehicles. *IEEE Transactions on Industry Applications*, 59(2), 2061-2068. <https://doi.org/10.1109/TIA.2022.3223631>
- [3] Ionescu, V. M., Săpunaru, A. A., Popescu, C. L., & Popescu, M. O. (2019). EMC norms for testing electric and hybrid cars. *Electric Vehicles International Conference (EV)*, 1-4. <https://doi.org/10.1109/EV.2019.8892881>
- [4] Podgorny, A. S., Nikolaev, P. A., & Kozlovskii, V. N. (2023). Standard approaches to ensuring the electromagnetic compatibility of vehicles. *Russian Engineering Research*, 43(8), 991-996. <https://doi.org/10.3103/S1068798X23080257>
- [5] Supa Stölben, I. R., Bertelmann, J., Beltle, M., Tenbohlen, S., Bersch, C., & Spanos, K. (2022). Investigation of ground impedances affecting EMC during charging operations of electric vehicles. *International Symposium on Electromagnetic Compatibility - EMC Europe*. <https://doi.org/10.1109/EMCEurope51680.2022.9900978>
- [6] Kozan, M. D. & Usta, E. (2019). EMC test requirements for electric vehicles. *Fifth International Electromagnetic Compatibility Conference*. <https://doi.org/10.1109/EMCTurkiye45372.2019.8976016>
- [7] Weng, Y., Chen, G., Jia, Z., Dong, A., & Su, D. (2022). Research on electromagnetic susceptibility test and analysis for the electric vehicle. *International Conference on Microwave and Millimeter Wave Technology (ICMMT)*. <https://doi.org/10.1109/ICMMT55580.2022.10022572>
- [8] Kroner, D., Lundgren, U., Augusto, A., & Bollen, M. (2024). Radiated electromagnetic emission from photovoltaic systems: Measurement results: Inverters and modules. *Energies*, 17(8), 1893. <https://doi.org/10.3390/en17081893>
- [9] Grazian, F., Shi, W., Dong, J., Van Duijzen, P., Soeiro, T. B., & Bauer, P. (2019). Survey on standards and regulations for wireless charging of electric vehicles. *AEIT International Conference of Electrical and Electronic Technologies for Automotive*, 1-5. <https://doi.org/10.23919/EETA.2019.8804573>
- [10] Pawar, S. P. & Desai, M. M. (2024). Electromagnetic compatibility (EMC) analysis for e-motors and controllers of electric two-wheelers. *Symposium on International Automotive Technology*. <https://doi.org/10.4271/2024-26-0098>
- [11] Gao, F., Ye, C., Wang, Z., & Li, X. (2018). Improvement of low-frequency radiated emission in electric vehicle by numerical analysis. *Journal of Control Science and Engineering*, 5956973. <https://doi.org/10.1155/2018/5956973>
- [12] Chudy, A. & Stryczewska, H. D. (2020). Electromagnetic compatibility testing of electric vehicles and their chargers. *Informatyka Automatyka Pomiary W Gospodarcei Ochronie Środowiska*, 10(3), 70-73. <https://doi.org/10.35784/iapgos.1687>
- [13] Reinhardt, U., Mooser, J., & Artz, T. (2015). Testing of high voltage systems installed in hybrid and electric vehicles. *IEEE International Symposium on Electromagnetic Compatibility (EMC)*. <https://doi.org/10.1109/ISEMC.2015.7256243>
- [14] Mastoi, M. S., Zhuang, S., Munir, H. M., Haris, M., Hassan, M., Alqarni, M., & Alamri, B. (2023). A study of charging-dispatch strategies and vehicle-to-grid technologies for electric vehicles in distribution networks. *Energy Reports*, 9, 1777-1806. <https://doi.org/10.1016/j.egyr.2022.12.139>
- [15] Săpunaru, A. A., Ionescu, V. M., Popescu, M. O., & Popescu, C. L. (2019). Study of radiated emissions produced by an electric vehicle in different operating modes. *Electric Vehicles International Conference (EV)*, 1-5. <https://doi.org/10.1109/EV.2019.8893142>
- [16] Mehrotra, S., Ray, R., Pandey, D., & Naithani, H. (2024). Comparison between state of art performance of GaN and SiC converters for electric vehicle application. *SAE Technical Paper*; 2024-26-0134. <https://doi.org/10.4271/2024-26-0134>
- [17] Mariscotti, A. (2022). Harmonic and supraharmonic emissions of plug-in electric vehicle chargers. *Smart Cities*, 5(2), 496-521. <https://doi.org/10.3390/smartcities5020027>
- [18] Dawson, L., Rowell, A., Armstrong, R., Ruddle, A., Addin, I., Melendez, J., & Galarza, A. (2014). *EMC design guidelines for manufacturers of vehicle electric drives (Deliverable D6.1-1.0)*. Electrical Powertrain Health Monitoring for Increased Safety of FEVs, European Commission, Seventh Framework Programme (FP7) - Green Cars.

- [19] Lunca, E., Vornicu, S., & Sălceanu, A. (2023). Numerical and analytical analysis of the low-frequency magnetic fields generated by three-phase underground power cables with solid bonding. *Applied Sciences*, 13(10), 6328. <https://doi.org/10.3390/app13106328>
- [20] Liu, X., Grassi, F., Spadacini, G., & Pignari, S. A. (2021). Toward a more realistic characterization of hand-assembled wire bundles: Geometrical modeling and EMC prediction. *IEEE Access*, 9, 129502-129511. <https://doi.org/10.1109/ACCESS.2021.3113767>
- [21] Wu, X., Zhang, Y., Wang, L., Chen, Q., Li, H., & Zhao, M. (2025). A simple cable radiated emission evaluation method for table-top setups according to CISPR 11 and CISPR 32. *IEEE Access*, 13, 19040-19048. <https://doi.org/10.1109/ACCESS.2025.3532460>
- [21] Basyigit, I. B., Dogan, H., & Helhel, S. (2019). The effect of aperture shape, angle of incidence and polarization on shielding effectiveness of metallic enclosures. *Journal of Microwave Power and Electromagnetic Energy*, 53(2), 115-127. <https://doi.org/10.1080/08327823.2019.1607496>
- [22] Güler, S. (2023). An investigation on electromagnetic shielding effectiveness of metallic enclosure depending on aperture position. *Journal of Microwave Power and Electromagnetic Energy*, 57(2), 129-145. <https://doi.org/10.1080/08327823.2023.2209477>

Contact information:**Sunay GÜLER**

FEV Türkiye,

Istanbul, Türkiye, 34469

E-mail: guler_s@fev.com; sunay.guler@hotmail.com